Torsional Potentials of Simple Polysilane Derivatives

C. X. Cui,[1a] A. Karpfen,[1b] and M. Kertesz*,[1a,c]

Department of Chemistry, Georgetown University, Washington, D.C. 20057, and the Institute for Theoretical Chemistry, University of Vienna, A-1090, Vienna, Austria

Received January 8, 1990; Revised Manuscript Received January 29, 1990

ABSTRACT: Torsional potential curves for simple infinite polysilane derivatives are calculated by various ab initio and semiempirical crystal orbital methods. The comparison includes polysilane, poly(difluorosilane), poly(methylsilane), poly(dimethylsilane), and poly(diethylsilane) and the two simplest carbon analogues polyethylene and poly(tetrafluoroethylene) as well as polygermane. Generally, the potential curves are more flat going from the carbon compounds to the silicon compounds. For polysilane the all-trans conformation is comparable or less stable in energy than the gauche conformation. The addition of bulkier side groups locks in the all-trans conformation relative to the gauche conformation. Connection of energetic with the thermochromic properties of polysilanes is discussed. A vibrational analysis and the corresponding phonon dispersion curves of polysilane with both all-trans and helical conformations are given for the first time.

High molecular weight silane polymers[2] are of interest due to their spectroscopic and semiconducting properties,[3] not to speak of their potentially valuable practical applications.[4] Progress in their research has reached the stage that fundamental structural issues are being raised.[5-7] Empirical force field calculations have been applied to model systems of polysilane such as H–$(SiH_2)_n$–H and poly(dimethylsilane) [Me–$(SiMe_2)_n$–Me][5a] (n up to 5) and to phenyl derivatives.[5b] The energetics of various conformers of the simple finite clusters of polysilane with n = 2–5 has been extensively studied with ab initio methods by Ortiz and Mintmire.[6] The energetics of an infinite polysilane has been calculated also with ab initio methods by Teramae and Takeda[7a] and with semiempirical quantum chemistry by two of the present authors.[7b]

In this paper we present our comparative studies of simple substituted polysilanes with substituents such as fluorine, methyl, and ethyl. We also compare our calculations with similar ones on corresponding carbon main chain polymers. Our calculations are based on an array of quantum chemical methods including various basis set ab initio work and semiempirical geometry optimizations. We also investigate the importance of full-geometry optimizations, which turns out to be less significant for the silicon compounds than for the carbon chains due to the fact that their potential curves are more flat. In our studies we will not devote too much room to other aspects of the microscopic calculations[8,9] but we will make some comments on the vibrational properties of polysilane and on the HOMO–LUMO gap which plays an important role in the now famous thermochromism of polysilanes.[10]

Methods

In all calculations a screw axis of symmetry has been taken into account. Calculations for polymers using translational symmetry and the "crystal orbitals" based on this symmetry are widespread.[11] In the presence of a screw axis of symmetry, the translation is accompanied by a rotation by the helical angle, θ, as shown in Figure 1. If the basis set orbitals are rotated together with the atoms they are associated with, the crystal orbitals resulting from this symmetry can be handled with straightforward modifications of the corresponding computer code.[7b,11b] Concerning the semiempirical calculations, more details have been given recently.[7b] As to the ab initio calculations, the calculational procedures follow those of ref 11a. The basis sets and parameterizations are identified in the corresponding tables. AM1[12d] is a version of the MNDO (modified neglect of diatomic overlaps[12a]) semiempirical Hamiltonian.

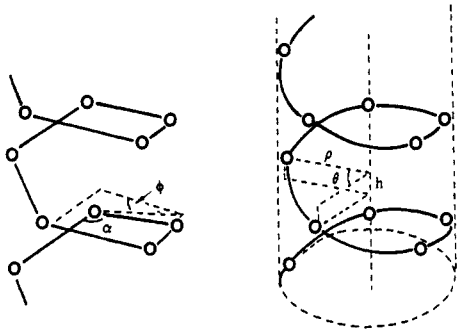

Figure 1. Atoms in a polymer with a screw axis of symmetry that is parallel to the z axis. θ is the helical angle, and ϕ is the dihedral angle of the consecutive bonds along the main chain of the polymer. Side groups can be attached to any atom: these are not shown for clarity.

Because the AM1 approach underestimates the rotational barrier around the single bonds although the conformation can be correctly predicted, a comparison of the results of the AM1 and ab initio calculations appears more appropriate in dealing with the rotation barriers. Such comparison is made frequently throughout this paper.

In what follows we first discuss the results of groups of systems and make overall comparison at the end.

The methodological aspects of the vibrational analysis will be given in the last section.

Polysilane and Polyethylene

In Table I we have summarized the optimized geometries of the all-trans conformation (θ = 180°) of polysilane using three different basis sets (MIDI-1, MIDI-1*, and 3-21G*) and the AM1 crystal orbital method. For comparison, we have included Ortiz and Mintmire's 3-21G* results from an Si_5H_{12} cluster, Mintmire's ab initio local density functional results for the infinite chain, and the double-ζ (DZ) results of Teramae and Takeda.[7a] Table II summarizes the available geometrical data of the optimized gauche conformation of $(SiH_2)_x$. Some of the larger basis set calculations are missing from this table, because

0024-9297/90/2223-3302$02.50/0

Table I
Optimized Geometrical Parameters[a] of *all-trans*-Polysilane Using Different Crystal Orbital Methods

	MIDI-1[b]	MIDI-1*[c]	3-21*[d]	AM1[e]	DZ[f]	3-21G* (cluster)[g]
r_{Si-Si}	2.383	2.372	2.344	2.395	2.382	2.347
r_{Si-H}	1.487	1.491	1.481	1.471	1.485	1.481
∠SiSiSi	112.4	112.1	111.9	107.4	112.4	112.2
∠HSiH	107.8	107.5	108.0	109.31	107.8	107.4

[a] Bond distances in angstroms (1 Å = 10^{-10} m), angles in degrees. All data correspond to fully optimized geometry unless noted otherwise. [b] See ref 13a. [c] See ref 13b. [d] See ref 13c. [e] See refs 12 and 7b. [f] See ref 7a; DZ = double-ζ basis set. [g] Based on the middle part of an Si_6H_{12} cluster.[6a]

Table II
Optimized Geometrical Parameters[a] for the Gauche Conformation of Polysilane Using Different Methods

	MIDI-1[b]	AM1[c]	3-21G*(cluster)[d]
r_{Si-Si}	2.383	2.390	2.346
r_{Si-H}	1.487[e]	1.475	1.481
∠SiSiSi	111.1	107.9	110.5
∠HSiH	107.8[e]	108.6	
θ[f]	96.8	83.9	
ϕ[f]	73.9	46.3	73.5

[a] See *a* in Table I. [b] See *b* in Table I. [c] See ref 12d for parameters and ref 7b for method of calculation. [d] Taken from ref 6a (data of Si_6H_{12}). [e] Optimized only at $\theta = 180°$ (all-trans conformation). [f] θ is the helical (or screw) angle, and ϕ is the SiSiSiSi dihedral angle (see Figure 1).

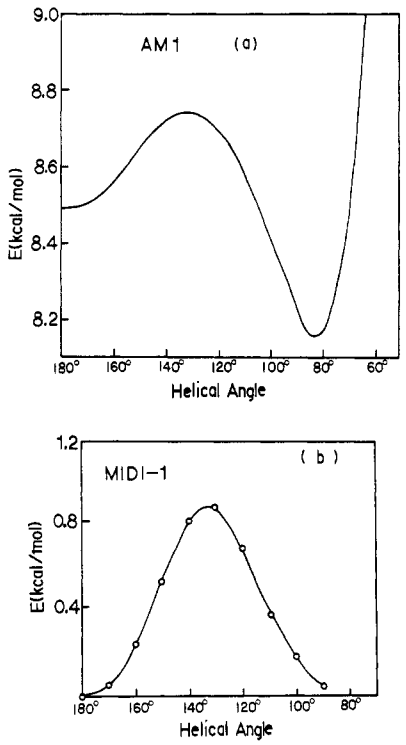

Figure 2. Torsional potential of polysilane using (a) fully optimized AM1 crystal orbital calculation and (b) rigid rotor MIDI-1 crystal orbital calculation (geometry optimized at $\theta = 180°$).

at smaller helical angles the structure becomes more compact; i.e., the helix coils back and atoms far along the main chain come in close contact. This necessitates the inclusion of many more neighbors in the calculations (easily up to 15), and the computation becomes prohibitively expensive with the present version of the ab initio program. However, as we shall see shortly, due to the large variety of data available, we can estimate the results of these calculations well. In Figure 2 we show the energy per chemical repeat unit of the polymer as a function of the helical angle. (For ab initio calculations the energy relative to the most stable conformation is given; for MNDO or AM1, the heat of formation is given.) Such

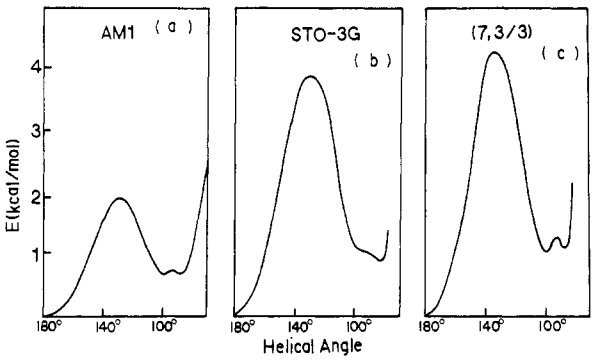

Figure 3. Torsional potential of polyethylene: (a) fully optimized AM1; (b) fully optimized STO-3G (after ref 11b); (c) rigid rotor (7,3/3) (after ref 11b).

torsional potentials can be produced in essentially two major variants: either all bond distances, bond angles, and dihedral angles are optimized for each value of θ (fully optimized calculation) or all such geometrical parameters are kept fixed except those dihedral angles that determine the helix along the main chain of the polymer ("rigid rotor" (RR) calculation). Partial optimizations, of course, are also practical and may yield results close to the fully optimized ones, once it has become clear which geometrical parameters couple mostly to the torsional deformation. As a comparison, the torsional potential curves of polyethylene calculated by the AM1 semiempirical method and ab initio approach at the STO-3G and (7,3/3) level are presented in Figure 3. The rotation barrier by the AM1 approach is underestimated by ca. 2 kcal/mol.

Poly(difluorosilane) $[(SiF_2)_x]$ and Poly(tetrafluoroethylene) $[(CF_2)_x]$

Although from a chemical point of view these two systems are much more ionic than the parent compounds, they seemed to be the next logical pair in the series of substituted derivatives to investigate. Due to the increased size and ionicity of the side group, significant changes occur in the relative energetics of the trans and gauche conformations. Figure 4 shows the rigid rotor torsional potential curve for $(SiF_2)_x$ and the fully optimized AM1 curve. In Figure 5 similar data plus fully optimized MIDI-1 points are given for the carbon analogue, $(CF_2)_x$. The geometrical data corresponding to the two local minima are summarized in Table III. While there is good agreement between the two conformations for the carbon compound, significant differences occur for the silicon compound.

It is a well-known feature of the torsional potential curve of $(CF_2)_x$ that one of the minima is at $\theta < 180°$, not at $\theta = 180°$.[14] All our quantum chemical calculations agree with this empirical finding, as did the RR calculation of Otto et al.[15,16] It is tempting to blame the larger size of the fluorine relative to the hydrogen on this shift, but the situation is more complex: the C–C bond distance actually shrinks by ca. 0.02 Å at the MIDI-1 level, in agreement with general experimental trends.[10]

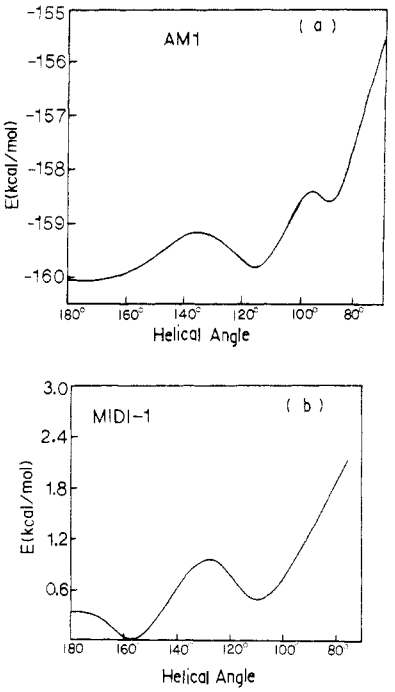

Figure 4. Torsional potential of poly(difluorosilane) $[(SiF_2)_x]$: (a) fully optimized AM1; (b) rigid rotor MIDI-1 geometry optimized at $\theta = 180°$.

It has been suggested in the early literature that the torsional potential of $(CF_2)_x$ ought to have three minima: one close to the all-trans conformation ($\phi \approx 165$–$170°$) and two gauche conformations ($\phi \approx 120°$ and $\phi \approx 60°$). As mentioned before, calculations at the ab initio level are difficult around $\theta = 60°$. Since the torsional potentials as a function of the helical angle θ are somewhat compressed around $\theta \approx 60°$ (which corresponds to $\phi = 0°$), the third minimum does not fully show on the STO-3G fully optimized torsional potential curve of $(CF_2)_x$, although it is clearly present, since the energy is very high at $\theta = 60°$ by definition. In the larger MIDI-1 basis set the third minimum cannot be located, because the calculation does not converge below $\theta = 90°$.

The corresponding AM1 potential qualitatively agrees with the ab initio and the empirical results. Two minima are around $\theta \approx 170°$ and 110°, and a third shallow minimum is at 85°. The barrier between the first two minima is ~2.5 kcal/mol, and the minima are close in energy. The fully optimized ab initio barrier is ca. 2 times higher. The third minimum cannot be compared with the ab initio result (we have no fully optimized data for it, for the reason mentioned above). Indications are, however, that the AM1 result for this minimum is reasonable as to both its location and relative energy.

The results for $(SiF_2)_x$ parallel those for $(CF_2)_x$ as to the location and relative heights of the minima. Here, only part of the RR ab initio curve is available using the MIDI-1 basis set, with the geometry optimized only at $\theta = 180°$. The third minimum could not be studied, because of the convergence troubles mentioned before. The AM1 results show three minima around $\theta = 170°$, 115°, and 90°. The barrier between the first two is reduced relative to polyethylene to <1 kcal/mol.

Poly(methylsilane), Poly(dimethylsilane), and Poly(diethylsilane)

For the rest of the compounds with larger side groups only fully optimized AM1 crystal orbital results are available.

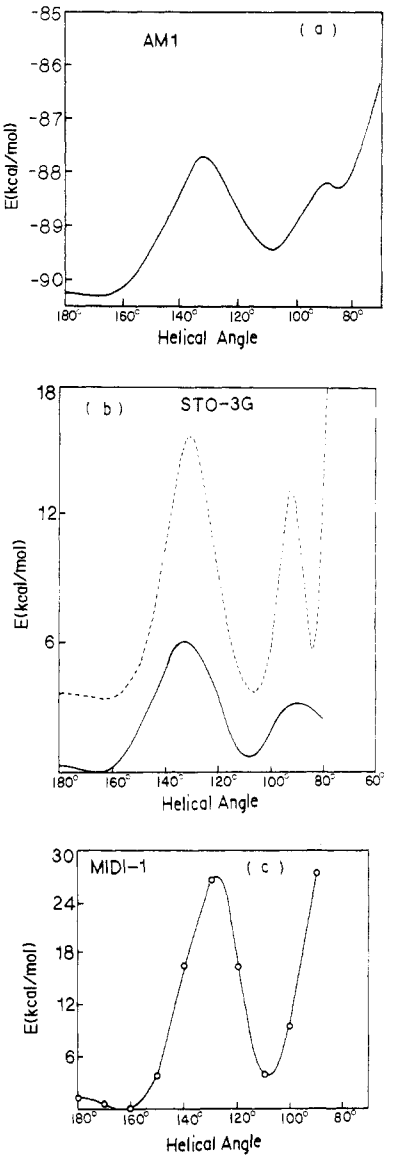

Figure 5. Torsional potential of poly(tetrafluoroethylene): (a) fully optimized AM1; (b) STO-3G [(- - -) rigid rotor (RR); (—) fully optimized]; (c) rigid rotor MIDI-1 (geometry optimized at $\theta = 180°$).

The corresponding torsional potentials are given in Figure 6. The following trend can be observed relative to polysilane. With the growing size and growing number of side groups, (a) the all-trans conformation becomes more stable than the gauche conformation and (b) the barrier separating the two conformations is also substantially increasing. Both changes amount to locking in the trans conformation more and more as the size and number of side groups increase. The trend with fluorine substitution is quite similar. This effect of locking in one structure is primarily due to the steric hindrances of the side groups, which make the chain stiffer as they "crowd" along the main chain. Others, e.g., Welsh et al.[5b] and Damewood,[5d] have also noted this effect.

Comments on Thermochromism

Thermochromism of polysilanes has been attributed to conformational changes of the polymer backbone. As the temperature is raised, random deviations will occur from the lowest energy configuration, be it around the planar all-trans or the helical gauche. However, thermochromism is more readily compatible with the planar ground state than with a gauche, for the following rea-

Table III
Optimized Geometrical Parameters[a] for the Near-All-Trans and the Lowest Gauche Conformations of $(CF_2)_x$ and $(SiF_2)_x$

	$(CF_2)_x$ (X = C)			$(SiF_2)_x$ (X = Si)		
	MIDI-1[b]	AM1		MIDI-1	AM1	
r_{X-X}	1.527[b]	1.611[c]	1.615[d]	2.319[b]	2.590[c]	2.596[d]
r_{X-F}	1.364[b]	1.368[c]	1.368[d]	1.632[b]	1.623[c]	1.623[d]
∠XXX	115.7[b]	110.0[c]	112.1[d]	107.6[b]	99.8[c]	99.1[d]
∠FXF	110.3[b]	104.3[c]	103.6[d]	123.1[b]	103.8[c]	103.4[d]
θ_{trans}	170	175		160	168	
θ_{gauche}	109	110		100	118	

[a] See note *a* in Table I. [b] Optimized only at $\theta = 180°$ (all trans). [c] Value given corresponds to the optimized all-trans conformation. [d] Value given corresponds to the optimized all-gauche conformation.

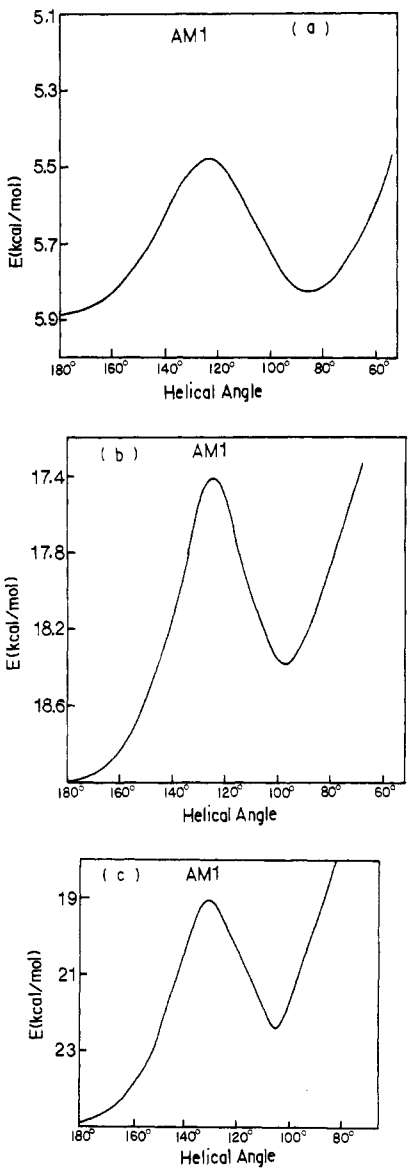

Figure 6. Torsional potential of alkyl-substituted polysilanes by the fully optimized AM1 method: (a) poly(methylsilane); (b) poly(dimethylsilane); (c) poly(diethylsilane).

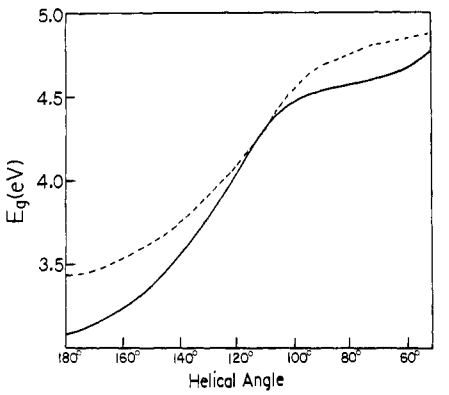

Figure 7. Energy gap (E_g) of (a) polysilane (—) and (b) poly(dimethylsilane) (– – –) as a function of the helical angle θ (EHT calculation, based on the AM1 optimized geometry).

sons. First, let us look at the variation of the energy gap, E_g, as a function of θ (Figure 7). For this purpose, extended-Hückel theory (EHT) results are given, since these are much more reasonable than either the ab initio or the MNDO (AM1) results.[7b] (The following EHT parameters of Si were used: exponents of s, p, and d orbitals are 1.63, 1.43, and 1.383, respectively, and ionization energies of the corresponding orbitals are −17.3, −9.20, and −3.0. For carbon and hydrogen standard parameters are used.[7b]) The increase of the gap relative to its minimum at the all-trans configuration is obviously due to the loss of σ-conjugation, similarly to the case of polythiophene.[17] As the temperature is raised, the neighboring units move away from their energetically optimal position in a random fashion. Therefore, the screw axis of symmetry is lost, and our calculations cannot be directly applied to such a situation. However, assuming a rough additivity of the total energy, we may comment on what to expect upon raising the temperature. A distribution of θ values is expected. Small deviations from the $\theta = 180°$ values would result in a broadening of the absorption and an accompanying shift. The order of magnitude of this shift can be estimated by using a Boltzmann distribution of θ values in connection with the $E(\theta)$ curve. Thus, for instance, for poly(dimethylsilane), at room temperature θ values between 180° and 150° would be strongly occupied. Looking at the E_g vs θ curve on Figure 7, we would expect a distribution of E_g values between 3.1 and 3.5 eV as opposed to a single E_g value at very low temperatures at 3.1 eV. This shift is too small to account for the experimentally observed blue-shift values ($\simeq$0.5–0.7 eV). Another problem with this model is that it predicts a smooth shift without a sharp transition. The direction of the shift agrees with the experiments.

Another alternative is that a melting of the side groups allows θ values to deviate more significantly from the $\theta \approx 180°$ region up to the region of $\theta \approx 110$–90° (gauche conformation). Such conformations, using Figure 7 for estimating the gap shift, would amount to a shift of 1.0–1.4 eV. The same calculated shifts for the dimethyl compound are even smaller: 0.9–1.2 eV. This agrees better with the observed sharp transition and shift. Also, we must stress again that the $E_g(\theta)$ curve is based on an idealized uninterrupted perfect helix and yields therefore an upper estimate of the shift.

Let us make a comment on polygermane, whose MNDO torsional potential is shown in Figure 8. As expected by simple size arguments, this displays the flattest curve out of the three hydrides considered and amounts to practi-

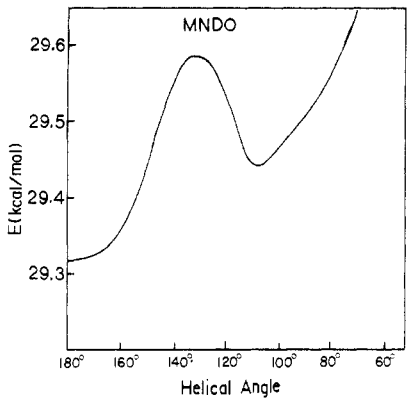

Figure 8. Fully optimized torsional potential of $(GeH_2)_x$ using the MNDO parametrization.

Table IV
Comparison of Experimental and Calculated Vibrational Frequencies (cm^{-1}) with Force Constant Scaling for Si_2H_6

frequency		
exptl[a]	calcd[b]	error
379	415.5	-36.5
379	415.5	-36.5
432	431.6	0.4
628	592.6	35.4
628	592.6	35.4
844	874.8	-30.8
920	893.8	26.2
940	940.3	-0.3
940	940.4	-0.4
941	943.9	-2.9
941	944.0	-3.0
2154	2168.1	-14.1
2155	2168.1	-13.1
2155	2168.4	-13.4
2163	2168.4	-5.4
2179	2171.4	7.6
2179	2175.6	3.4

[a] Reference 20a. [b] Calculated frequency based on scaled force constants (AM1).

cally free rotation at room temperature from the all-trans to the all-gauche conformation. We have also carried out an AM1 calculation on polygermane, which displays also a flat potential, although the relative stability of the trans and gauche conformations is reversed.

Vibrational Analysis of Polysilane

As a byproduct of our energy minimizations, we also obtained force constants for the silicon polymers in question. However, the process to obtain vibrational frequencies from these data presents three problems. One difficulty is the well-known fact that force constants from quantum chemical calculations have to be empirically scaled.[18] Second, the force constants emanating from quantum chemical calculations based on crystal orbitals, such as the ones described in the previous parts of this paper, are based on strict translational symmetry and therefore correspond to "frozen phonons"[19a] at $k = 0$. Therefore, only a fixed linear combination of the force constants can be obtained, which makes it impossible to determine the $k \neq 0$ vibrational energies ("phonon dispersion curves").[19b] Third, the screw axis of symmetry presents a further complication. This latter problem can be solved in a straightforward manner by using the screw axis of symmetry in generating the symmetry-adapted vibrational coordinates of the polymer. This necessitates the use of rotated x and y displacement coordinates (if the screw is along the z axis). The similarity with the electronic problem is obvious and will be discussed separately at length elsewhere.[19c]

We overcame the first two difficulties by employing a cluster approach. Obviously, in a cluster, Pulay's force constant scaling strategy[18] can be directly applied. The results of the scaling factor fitting for Si_2H_6 are given Table IV. The corresponding scaling factors and force

Table V
Comparison of Selected Force Constants (FC) for $(SiH_2)_x$ from AM1 Calculations on Si_7H_{16} with the Available Experimental Data

descrip	scaling factor	scaled FC	exptl for Si_2H_6
Si-H str	0.9447	2.652	2.692
Si-Si str	1.1081	1.746	1.838
H-Si-Si bending	1.5588	0.564	0.396
H-Si-H bending	1.3602	0.617	0.436
Si-Si-Si bending[a]	1.5210	0.562	
Si-Si-Si-Si tors[b]	1.0000	0.294	
Si-Si-Si-H tors[c]	1.3602	0.479	
H-Si-Si-H[d]	1.3602	0.288	

[a] From fitting of the Si-Si-Si bending vibration in Si_3H_8.[20b] [b] Assumed value, not varied during fitting. [c] Assumed to be identical with the H-Si-Si-H scaling factor for Si_2H_6. [d] Optimized for Si_2H_6.[20a]

Table VI
Comparison of Calculated Vibrational Frequencies by Crystal Orbital and Oligomer Approaches (AM1, without Scaling) for *all-trans*-Polysilane

species	CO[a]	MO(III)[b]	MO(II)[c]	MO(I)[d]	vib mode
I	2214.06	2215.21	2215.18	2215.56	SiH_2 sym str (A_g)
II	2209.49	2209.63	2209.61	2209.99	SiH_2 sym str (B_{2u})
III	2207.43	2208.98	2208.95	2208.54	SiH_2 asym str (B_{3g})
IV	2205.89	2208.00	2207.96	2207.56	SiH_2 asym str (B_{1u})
V	763.69	762.99	762.88	762.68	SiH_2 bending (A_g)
VI	758.82	758.00	757.89	757.69	SiH_2 bending (B_{2u})
VII	610.39	607.41	608.89	614.82	SiH_2 wagging (B_{1g})
VIII	544.71	543.79	543.88	544.47	SiH_2 twisting (B_{2g})
IX	524.32	523.82	525.30	529.86	Si-Si str (B_{3u})
X	447.72	446.84	447.15	454.52	SiH_2 wagging (B_{1g})
XI	416.74	415.44	415.44	416.19	SiH_2 twisting (A_u)
XII	416.51	415.25	415.34	414.62	SiH_2 rocking (B_{3g})
XIII	381.05	379.93	380.25	377.92	Si-Si str (A_g)
XIV	271.76	268.42	268.45	267.47	SiH_2 rocking (B_{1u})

[a] The crystal orbital method combined with the frozen-phonon approach.[12b] [b] The force constants have been obtained from Si_7H_{16} and the third nearest neighbors have been included in the calculations. [c] The same strategy as (III) except for the second nearest neighbors involved. [d] The same strategy as (III) and the nearest-neighbor approach.

Table VII
Calculated and Experimental Vibrational Spectra of Polysilane (cm^{-1})

	obsd			
species	IR[a]	Raman[b]	calcd[c]	assign
I (A_g)	inactive	2155	2153	sym str
II (B_{2u})	2100	inactive	2147	sym str
III (B_{1u})	2100	inactive	2146	asym str
IV (B_{3g})	inactive	2115	2146	asym str
V (A_g)	inactive	909	907	bending
VI (B_{2u})	905 (890)[d]	inactive	904	bending
VII (B_{1g})	inactive		736	wagging
XI (B_{2g})	inactive	630	668	twisting
IX (B_{3u})	(845)[d]	inactive	642	wagging
VIII (A_u)	inactive	inactive	518	twisting
XIV (B_{3g})	(690)[d]		482	rocking
X (B_{1g})	inactive	480	473	Si-Si str
XIII (A_g)	inactive		414	Si-Si str
XII (B_{1u})		inactive	318	rocking

[a] Reference 22. [b] Reference 21. [c] *all-trans*-Polysilane. [d] From ref 22b.

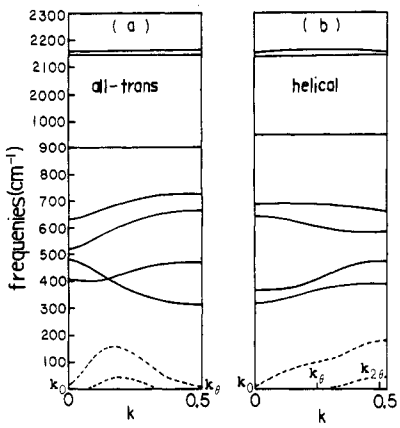

Figure 9. Vibrational (phonon) dispersion curves for (a) *all-trans*-polysilane (here, $k_{2\theta} = k_0$) and (b) helical *gauche*-polysilane using empirically scaled AM1 force constants. The dashed lines correspond to the low-energy acoustic modes. k_0, $k_{1\theta}$, and $k_{2\theta}$ correspond to spectroscopically active modes.

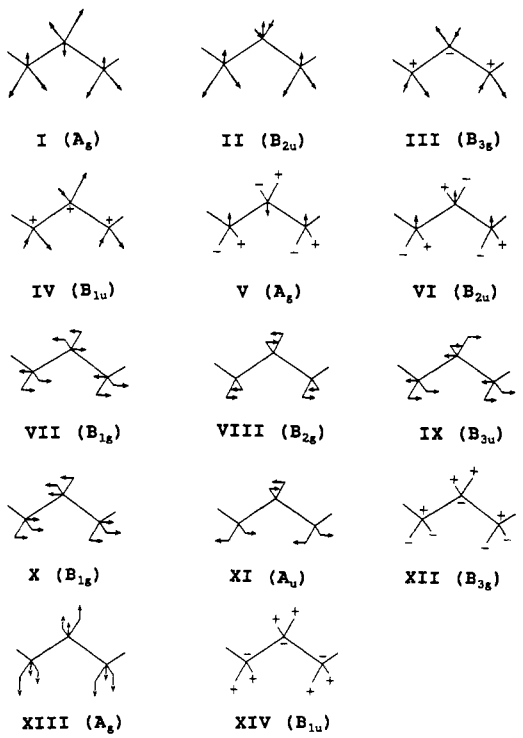

Figure 10. Vibrational modes of *all-trans*-polysilane.

constants are given in Table V. In all further calculations these scaling factors were kept unchanged, and all force constants were scaled by Pulay's method.[18] As a next step we used a finite cluster fragment of polysilane, Si_7H_{16}, for both the all-trans and the all-gauche configurations. This allowed us to obtain force constants up to the third atomic neighbor (relative to the central atom). Table VI demonstrates that the cluster approach is sufficiently accurate in reproducing the results of the more accurate "frozen-phonon" results. Of course, in this comparison, no scaling was used. Clearly, the inclusion of the third-neighbor forces leads to a duplication of the results from the frozen-phonon approach (see column 3 in Table VI).

The final scaled, third-neighbor phonon calculations are summarized in Table VII and Figures 9 and 10. Selection rules for the IR- and Raman-allowed transitions for translationally symmetrical polymers ($\theta = 0$ or 360°) are well-known: only modes at $k_0 = 0$ can be active.[23] For helical polymers, the situation is more complex: From group theory it can be demonstrated that in addition to the $k_0 = 0$ modes, other modes at $k_\theta = \theta/h$ may be both IR- and Raman-active and at $k_{2\theta} = 2\theta/h$ may be Raman-active. (If $k_{1\theta}$ or $k_{2\theta}$ would fall outside the $(-\pi/h, \pi/h)$ interval, $\pm 2\pi/h$ should be added.) Generally, the number of spectroscopically active modes for a given helical polymer will not depend on the order of the screw axis if the order is beyond 5.[19c] $k_{1\theta}$ and $k_{2\theta}$ are indicated in Figure 9, which was produced by a standard polymeric GF analysis.[19,20] The vibrational dispersions for *all-trans*- and *all-gauche*-$(SiH_2)_x$ are quite similar, but there is a clear difference around 900 cm^{-1}; the trans conformation fits the experiments better.[21,22] Observation of differences such as this may facilitate identification of various conformers of polysilane.

Acknowledgment. This research has been generously supported by a grant from the U.S. Air Force Office of Scientific Research (Grant 89-0229). We are indebted to Prof. P. Pulay for giving us his vibrational coordinate transformation program.

References and Notes

(1) (a) Georgetown University. (b) Institute for Theoretical Chemistry, Vienna. (c) Camille and Henry Dreyfus Teacher-Scholar (1984–1989).
(2) (a) West, R. *J. Organomet. Chem.* **1986**, *300*, 327. (b) Ziegler, J. M. *Synth. Met.* **1989**, *28*, C581.
(3) (a) Trefonas, P.; West, R.; Miller, R. D.; Hofer, D. *J. Polym. Sci., Polym. Lett. Ed.* **1983**, *21*, 823. (b) Pitt, C. G. In *Homoatomic Rings, Chains and Macromolecules of Main-Group Elements*; Rheingold, A. L., Ed.; Elsevier: New York, 1977. (c) West, R.; David, L. D.; Djurovich, P. I.; Stearley, K. L.; Srinivasan, K. S. V.; Yu, H. *J. Am. Chem. Soc.* **1981**, *103*, 7352. (d) Kepler, R. G.; Ziegler, J. M.; Harrah, L. A.; Kurtz, S. R. *Phys. Rev. B* **1987**, *35*, 2818. (e) Stolka, M.; Yuh, H.-J.; McGrane, K.; Pai, D. M. *J. Polym. Sci., Part A: Polym. Chem. Ed.* **1987**, *25*, 823.
(4) (a) West, R.; Wolff, A. R.; Peterson, D. J. *J. Radiat. Curing* **1986**, *13*, 35. (b) Hofer, D. C.; Miller, R. D.; Willson, C. G.; Neureuther, A. R. *Proc. of SPIE* **1984**, *469*, 108.
(5) (a) Damewood, J. R., Jr.; West, R. *Macromolecules* **1985**, *18*, 159. (b) Welsh, W. J.; Damewood, J. R., Jr.; West, R. C. *Macromolecules* **1989**, *22*, 2947. (c) Farmer, B. L.; Rabolt, J. F.; Miller, R. D. *Macromolecules* **1987**, *20*, 1161. (d) Damewood, J. R., Jr. *Macromolecules* **1985**, *18*, 1793.
(6) (a) Ortiz, J. V.; Mintmire, J. W. *J. Am. Chem. Soc.* **1988**, *110*, 4522. (b) Mintmire, J. W. *Mater. Res. Soc. Symp. Proc.* **1989**, *141*, 235. (c) Mintmire, J. W. *Phys. Rev. B* **1989**, *39*, 13350.
(7) (a) Teramae, H.; Takeda, K. *J. Am. Chem. Soc.* **1989**, *111*, 1281. (b) Cui, C. X.; Kertesz, M. *J. Am. Chem. Soc.* **1989**, *111*, 4216. (c) Takeda, K.; Teramae, H.; Matsumoto, N. *J. Am. Chem. Soc.* **1986**, *108*, 8186. (d) Takeda, K.; Matsumoto, N.; Fukuchi, M. *Phys. Rev. B* **1984**, *30*, 5871.
(8) (a) Bock, H.; Ensslin, W.; Feher, F.; Freund, R. *J. Am. Chem. Soc.* **1976**, *98*, 668. (b) Ernst, C. A.; Allied, A. L.; Ratner, M. A. *J. Organomet. Chem.* **1979**, *178*, 119. (c) Nelson, J. T.; Pietro, W. J. *J. Phys. Chem.* **1988**, *92*, 1365. (d) Michl, J.; Downing, J. W.; Karatsu, T.; Klingensmith, K. A.; Wallraff, G. M.; Miller, R. D. In *Inorganic and Organometallic Polymers*; Zeldin, M., Wynne, K. F., Allcock, H. R., Eds.; American Chemical Society: Washington, DC, 1988; p 61.
(9) (a) Seki, K.; Mori, T.; Inokuchi, H.; Murano, K. *Bull. Chem. Soc. Jpn.* **1988**, *61*, 351. (b) Herman, F. *Chem. Phys.* **1988**, *122*, 53.
(10) (a) References 2a and 3b. (b) West, R. In *Comprehensive Organometallic Chemistry*; Wilkinson, G., Stone, F. G. A., Abel, E. W., Eds.; Pergamon: Oxford, 1983; Vol. 9, p 365.
(11) (a) For a review, see, e.g.: André, J.-M. *Adv. Quantum Chem.* **1980**, *12*, 65. (b) Karpfen, A.; Beyer, A. *J. Comput. Chem.* **1984**, *5*, 11.
(12) (a) Dewar, M. J. S.; Thiel, W. *J. Am. Chem. Soc.* **1977**, *99*, 4899, 4907. (b) Stewart, J. P. *QCPE Bull.* **1985**, *5*, 62; *MOSOL Manual*; USAF: Colorado Springs, CO, 1984. (c) Lee, Y.; Kertesz, M. *J. Chem. Phys.* **1988**, *88*, 2609. (d) Dewar, M. J. S.; Thiel, W. *J. Am. Chem. Soc.* **1985**, *107*, 3902. (e) Dewar, M. J. S.; Jie, C. *Organometallics* **1987**, *6*, 1486; **1989**, *8*, 1544. (f) Fabian, W. M. F. *J. Comput. Chem.* **1988**, *9*, 369.
(13) MIDI-1 basis set: Huzinaga, S.; Tatewaki, H. *J. Comput. Chem.* **1980**, *1*, 205; Sakai, Y.; Tatewaki, H.; Huzinaga, S. *Ibid* **1981**, *2*, 100.

(14) (a) DeSantis, P.; Giglio, E.; Liquori, A. M.; Repanonti, A. J. Polym. Sci., Part A 1963, 1, 1383. (b) Magnasco, V.; Gay, G.; Nicora, C. Il Nuovo Cim. 1964, 34, 1263. (c) McCullogh, R. L.; McMahon, P. E. Trans. Faraday Soc. 1969, 69.
(15) Otto, P.; Ladik, J. J.; Förner, W. Chem. Phys. 1985, 95, 365.
(16) Brown, D. E.; Beagley, B. J. Mol. Struct. 1977, 38, 167.
(17) (a) Tourillon, G.; Garnier, F. J. Electroanal. Chem. 1984, 161, 51. (b) Cui, C. X.; Kertesz, M. Phys. Rev. B 1989, 40, 9661.
(18) (a) Pulay, P.; Fogarasi, G.; Dang, F.; Boggs, J. E. J. Am. Chem. Soc. 1979, 101, 2550. (b) Pulay, P.; Fogarasi, G.; Pongor, G.; Boggs, J. E.; Vargha, A. J. Am. Chem. Soc. 1983, 105, 7037.
(19) (a) Piseri, L.; Zerbi, G. J. Mol. Spectrosc. 1968, 26, 254. (b) Decius, J. C.; Hexter, R. M. Molecular Vibrations in Crystals; McGraw-Hill: New York, 1977. (c) Cui, C. X.; Kertesz, M., to be published.
(20) (a) Durig, J. R.; Church, J. S. J. Chem. Phys. 1980, 73, 4784. (b) Feher, F.; Fisher, H. Naturwissenschaften 1969, 51, 461.
(21) Vora, P.; Solin, S. A.; John, P. Phys. Rev. B 1984, 29, 3423.
(22) (a) John, P.; Odeh, I. M.; Thomas, M. J. K.; Wilson, J. I. B. J. Phys. (Paris) 1981, 4, C651. (b) Furukawa, S.; Matsumoto, N.; Toriyama, T.; Yabumoto, N. J. Appl. Phys. 1985, 58, 4658.
(23) (a) Higgs, P. W. Proc. R. Soc. London 1953, A220, 472. (b) Liang, C. Y. J. Mol. Spectrosc. 1957, 1, 61.

Registry No. $(SiF_2)_n$ (SRU), 31801-01-1; $(GeH_2)_n$, 32028-94-7; Si_2H_6, 1590-87-0; Si_7H_{16}, 14693-65-3; polysilane, 32028-95-8; polyethylene, 9002-88-4; poly(tetrafluoroethylene), 9002-84-0; poly(methylsilane), 110477-49-1; poly(dimethylsilane), 28883-63-8; poly(diethylsilane), 125457-34-3.

Rubberlike Network Structure from Tensile Tests on Swollen Samples According to Flory's Last Theory and Application to Polyurethanes

Mario Pegoraro,* Luca Di Landro, and Nanyung Cao

Dipartimento di Chimica Industriale e Ingegneria Chimica "G. Natta", Politecnico di Milano, p.zza L. da Vinci 32, 20133 Milano, Italy

Received August 2, 1989; Revised Manuscript Received November 28, 1989

ABSTRACT: It is shown that Flory's last elasticity theory allows calculation of the limit values for the network chain molecular weight starting from mechanical equilibrium measurements of the modulus $|f^*|$. For any case it is possible to evaluate the upper limit M_a corresponding to affine behavior. However, it is not always possible to evaluate the lowest limit: when M is known and the synthesis conditions are controlled, the lowest limit is M_s, which is the chain stoichiometric molecular weight; otherwise, the lowest limit becomes M_{ph}, corresponding to phantom behavior, which, however, can be calculated only when the effective functionality ϕ of the network cross-links is known. It is also shown that imperfections of the cross-linking reactions can be estimated by comparing the experimental modulus with that of the perfect phantom network characterized by the stoichiometric M_s and ϕ_s (eq 15). A practical example of this analysis is proposed for two classes of polyurethanes, polyether diols reacted with toluenediyl diisocyanate (TDI) and polyester diols reacted with TDI. The demonstrations and the applications are made in the case of a swollen system; however, they can be extended to dry systems simply by putting $v_2 = 1$ in the formulas.

General Considerations

Tensile testing of swollen samples has been employed for a long time as a method to evaluate the effective elastic chain density in rubber networks. The difficulty in properly modeling the network behavior has been responsible for the growth of different theories for describing the mechanical properties in relation to the chemical-physical structure of these materials.[1-3]

The more recent theory of Flory[4-7] has led to complex analytical expressions. Referring to a network deformed by an applied tensile force f corresponding to an elongation ratio α, one can write the following constitutive equation:[4,5]

$$f = \frac{\xi KT}{L_0}\left(\frac{V}{V_0}\right)^{1/3}(\alpha - \alpha^{-2})\left(1 + \frac{f_c}{f_{ph}}\right) = f_{ph}\left(1 + \frac{f_c}{f_{ph}}\right) \qquad (1)$$

where f_{ph} is the tensile response the network would give if deformed following the "phantom" model, which was originally proposed by James and Guth.[2] f_c is given by constraints acting on the fluctuating junctions due to the presence of "entanglements".[4-7] Equation 1 refers to a network at temperature T and volume V. ξ is defined as the cycle rank of the network, i.e., the number of independent circuits therein, K is the Boltzmann constant, and L_0 is the sample length at the reference volume V_0, which is defined as the volume at which the mean square end-to-end distance of the chains in the network is equal to that of the same chains in the free, un-cross-linked state. The reference volume V_0 is assumed to be the volume of the network at the moment of its formation at the same temperature T. In a previous theory[1,3] referring to a model where the relative displacement of junctions was assumed to be affine in the strain, the number ν of elastically effective chains was considered in place of the term $\xi(1 + f_c/f_{ph})$. The extent of entanglement constraints on junction fluctuations is, in general, dependent on the network deformation, so f_c is a function of α and V/V_0. Reasonable estimates of f_c/f_{ph}, supported by experiments,[7] show that f_c is usually positive, although it may present negative values at very high swelling ratios ($V/V_0 > 3.5$–4).

Let us examine a network initially formed at a volume V_o, for example, in solution, which is dried so that its

0024-9297/90/2223-3308$02.50/0